Int. J. Mech. Sci. Vol. 25, No. 11, pp. 803–809, 1983
Printed in Great Britain.

0020–7403/83 \$3.00 + .00
Pergamon Press Ltd.

SLIP BETWEEN A LAYER AND A SUBSTRATE CAUSED BY A NORMAL FORCE MOVING STEADILY OVER THE SURFACE

F. K. CHANG, MARIA COMNINOU and J. R. BARBER
Department of Mechanical Engineering and Applied Mechanics, University of Michigan, Ann Arbor, MI 48109, U.S.A.

(*Received* 28 *October* 1982; *in revised form* 21 *January* 1983)

Summary—A normal force moves slowly over the surface of a layer which is pressed against a substrate. Two asymmetric slip zones are generated if the force exceeds a friction dependent critical value. The slip is opposite in direction in the two zones, but due to the lack of symmetry, a net tangential shift of the layer is left behind by the passage of the force. This net shift is generally influenced by the coefficient of friction: for high coefficient, the layer shifts in the direction of motion, while for low coefficient, the shift is opposite. The latter result has been observed experimentally.

NOTATION

a	thickness of layer
$B(x)$	density of distributed glide dislocations
c	velocity of moving force
f	coefficient of friction
$h(x)$	tangential shift
N	normal tractions transmitted by contact interface
P	magnitude of normally applied concentrated force per unit thickness
p_0	initially uniform contact pressure between layer and substrate
S	shear tractions transmitted by contact interface
u_x, u_y	displacement components
$\hat{x}, \hat{y}$	fixed cartesian coordinates
x, y	cartesian coordinates in the moving system
κ	$3-4\nu$
μ	shear modulus
ν	Poisson's ratio
σ_{yy}, σ_{xy}	tractions of Flamant solution

INTRODUCTION

Recent studies of interface slip between an elastic layer and a substrate uniformly pressed together and subjected to a concentrated force[1–4] show that the direction of the applied force, the friction coefficient and whether the force is fixed or moving, influence significantly the characteristics of slip at the interface.

In static situations, tangential and normal forces have been studied separately[1–3]. For a tangential force[3], a slip zone first develops to the left of the force at the interface. As the force is slowly increased, a second slip zone appears and separation occurs inside the first slip zone, the order of these events depending on the magnitude of the coefficient of friction. For a normal force, two symmetric slip zones are formed at the interface and expand as the magnitude of the force increases[1, 2]. Separation also occurs eventually for a tensile force[2].

In moving situations, the tangential force has been considered in[4], assuming slow enough motion for inertia effects to be neglected. Two features emerge from the analysis as characteristic of the moving force. First, there is a net tangential shift in the direction of motion for the case considered in[4], and secondly the shear traction has a continuous derivative at the trailing end of the slip zone, in contrast to the familiar "hook" discontinuity of static problems.

In this paper we continue the study of moving forces, by considering a steadily moving normal force. This case merits special consideration since relevant experimental results are available[5]. Inertial effects are neglected and the analytical procedure of [4] is followed. It will be shown that as the force increases, slip starts simultaneously at two symmetric locations but the slip zones then expand asymmetrically.

FORMULATION

Consider the plane elasticity problem of a normal compressive force P per unit thickness moving with velocity c over the surface of an elastic layer, Fig. 1. We assume that c is sufficiently small for inertia effects to be neglected. The layer is pressed against a semi-infinite substrate of the same shear modulus μ and Poisson's ratio ν by a uniform pressure p_0. The thickness of the layer is denoted by a. Fig. 1 shows a co-ordinate system x, y which moves with the load at velocity c and is related to the fixed coordinate system $\hat{x}$, $\hat{y}$ by

$$x = \hat{x} - ct,\ y = \hat{y}. \tag{1}$$

If the loading parameter P/p_0a is sufficiently small, neither slip nor separation will occur at the interface and the interface tractions will be given by the static Flamant solution as

$$\sigma_{xy}(x, 0) = \frac{2P}{\pi}\frac{a^2x}{(a^2+x^2)^2} \tag{2}$$

$$\sigma_{yy}(x, 0) = -p_0 - \frac{2P}{\pi}\frac{a^3}{(a^2+x^2)^2}. \tag{3}$$

This condition will hold as long as the shear traction does not exceed the maximum static friction,

$$|\sigma_{xy}(x, 0)| < -f\sigma_{yy}(x, 0),\ \text{all } x \tag{4}$$

where f is the coefficient of friction. It is noted from (3) that the normal traction is always compressive. From equations (2) and (3) it follows that (4) will be violated in two symmetrically disposed regions if

$$P/p_0a > \frac{8\pi f[f(3+4f^2)^{1/2}+3+2f^2]^2}{27[(3+4f^2)^{1/2}-f]}. \tag{5}$$

We therefore anticipate the development of two slip zones $(-c_1, -b_1)$ and (b_2, c_2) as shown in Fig. 1.

Notice that although (2) and (3) give a symmetric violation of the inequality (4), the resulting slip zones will not generally be symmetric because the asymptotic conditions for the stick-slip transition are different for leading and trailing edges when the load is moving [4].

To take into account the slip zones we introduce a continuous distribution of glide dislocations with density $B(x)$. The same analytical procedure has been used in [1–4] and the reader is referred to [3] for further details. The total normal $N(x)$ and shear $S(x)$ tractions are

$$N(x) = -p_0 - \frac{2P}{\pi}\frac{a^3}{(a^2+x^2)^2} + \frac{2\mu}{\pi(\kappa+1)}\left[\left(\int_{-c_1}^{-b_1} + \int_{b_2}^{c_2}\right) B(\xi)K_n(x, \xi)\,d\xi\right] \tag{6}$$

$$S(x) = \frac{2P}{\pi}\frac{a^2x}{(a^2+x^2)^2} + \frac{2\mu}{\pi(\kappa+1)}\left[\left(\int_{-c_1}^{-b_1} + \int_{b_2}^{c_2}\right) B(\xi)K_s(x, \xi)\,d\xi\right] \tag{7}$$

where

$$K_n(x, \xi) = \frac{8a^3}{[4a^2+(x-\xi)^2]^2}\left[-3 + \frac{16a^2}{4a^2+(x-\xi)^2}\right] \tag{8}$$

$$K_s(x, \xi) = \frac{1}{x-\xi} - \frac{x-\xi}{4a^2+(x-\xi)^2} + \frac{12a^2(x-\xi)}{[4a^2+(x-\xi)^2]^2} - \frac{64a^4(x-\xi)}{[4a^2+(x-\xi)^2]^3}. \tag{9}$$

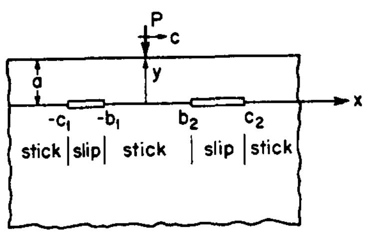

FIG. 1. Geometry and arrangement of slip zones.

The boundary conditions at the interface are

$$|S(x)| = f|N(x)|, \; -c_1 < x < -b_1, \; b_2 < x < c_2 \tag{10}$$

$$N(x) < 0, \text{ all } x \tag{11}$$

$$|S(x)| < f|N(x)|, \text{ outside the slip zones} \tag{12}$$

$$\operatorname{sgn} S(x) = \operatorname{sgn} \frac{dh}{dt} = sgn\, cB(x), \; -c_1 < x < -b_1, \; b_2 < x < c_2 \tag{13}$$

where $h(x)$ is the tangential shift due to the distributed dislocations defined as $h(x) = u_x(x, 0^+) - u_x(x, 0^-)$. It is related to the dislocation density by

$$B(x) = -\frac{dh}{dx}. \tag{14}$$

Anticipating the direction of slip from the Flamant solution, the boundary condition (8) in each slip zone can be rewritten

$$S(x) = fN(x), \; -c_1 < x < -b_1 \tag{15}$$

$$S(x) = -fN(x), \; b_2 < x < c_2 \tag{16}$$

and yields

$$\frac{2P}{\pi}\frac{a^2x}{(x^2+a^2)^2} + \frac{2\mu}{\pi(\kappa+1)}\left[\left(\int_{-c_1}^{-b_1} + \int_{b_2}^{c_2}\right) b(\xi)K_s(x, \xi \, d\xi\right]$$
$$= \rho\left\{-p_0 - \frac{2P}{\pi}\frac{a^3}{(x^2+a^2)^2} + \frac{2\mu}{\pi(\kappa+1)}\left[\left(\int_{-c_1}^{-b_1} + \int_{b_2}^{c_2}\right) B(\xi)K_n(x, \xi)\, d\xi\right]\right\} - c_1 < x < b_1, \; b_2 < x < c_2 \tag{17}$$

where

$$\rho = \begin{cases} f & -c_1 < x < -b_1 \\ -f & b_2 < x < c_2 \end{cases}. \tag{18}$$

The net tangential shift in each slip zone is

$$D_1 = \int_{-c_1}^{-b_1} B_1(\xi)\, d\xi, \; D_2 = \int_{b_2}^{c_2} B_2(\xi)\, d\xi \tag{19}$$

where

$$B(x) = \begin{cases} B_1(x) & -c_1 < x < -b_1 \\ B_2(x) & b_2 < x < c_2 \end{cases}. \tag{20}$$

The system of equations (17) involves four unknown parameters c_1, b_1, c_2, b_2 and two unknown functions $B_1(x)$ and $B_2(x)$. For the determination of these unknowns we have, in addition to (17), two equations that require $B_1(x)$ and $B_2(x)$ to be bounded functions and the inequalities (12) and (13). The latter are sufficient for the determination of the trailing edges of the slip zones as shown in[4].

NUMERICAL SOLUTION

To perform the numerical computations we first normalize the integration intervals by the change of variables

$$\xi_1/a = \delta_1 r_1 + \sigma_1 \quad x_1/a = \delta_1 s_1 + \sigma_1 \tag{21}$$

$$\xi_2/a = \delta_2 r_2 + \sigma_2 \quad x_2/a = \delta_2 s_2 + \sigma_2 \tag{22}$$

where

$$\delta_1 = (c_1 - b_1)/2a, \quad \sigma_1 = -(c_1 + b_1)/2a \tag{23}$$

$$\delta_2 = (c_2 - b_2)/2a, \quad \sigma_2 = (c_2 + b_2)/2a. \tag{24}$$

Equation (17) yields the following singular integral equations of the Cauchy type

$$\frac{1}{\pi}\int_{-1}^{1} \frac{B_1(r_1)}{r_1 - s_1} dr_1 + \frac{1}{\pi}\int_{-1}^{1} B_1(r_1)K_{11}(s_1, r_1)\, dr_1 + \frac{1}{\pi}\int_{-1}^{1} B_2(r_2)K_{12}(s_1, r_2)\, dr_2$$
$$= \frac{\kappa+1}{2\mu}\left\{p_0 f + \frac{2P}{\pi a}\frac{\delta_1 s_1 + \sigma_1 - f}{[(\delta_1 s_1 + \sigma_1)^2 + 1]^2}\right\}, \; -1 < s_1 < 1 \tag{25}$$

$$\frac{1}{\pi}\int_{-1}^{1}\frac{B_2(r_2)}{r_2-s_2}\,dr_2+\frac{1}{\pi}\int_{-1}^{1}B_2(r_2)K_{22}(s_2,r_2)\,dr_2+\frac{1}{\pi}\int_{-1}^{1}B_1(r_1)K_{21}(s_2,r_1)\,dr_1$$
$$=\frac{\kappa+1}{2\mu}\left\{-p_0f+\frac{2P}{\pi a}\frac{\delta_2s_2+\sigma_2-f}{[(\delta_2s_2+\sigma_2)^2+1]^2}\right\},\quad -1<s_2<1 \tag{26}$$

where

$$K_{11}(s_1,r_1)=\delta_1\left\{\frac{\delta_1(s_1-r_1)}{4+\delta_1^2(s_1-r_1)^2}-\frac{12[\delta_1(s_1-r_1)+2f]}{[4+\delta_1^2(s_1-r_1)^2]^2}+\frac{64[\delta_1(s_1-r_1)+2f]}{[4+\delta_1^2(s_1-r_1)^2]^3}\right\} \tag{27}$$

$$K_{22}(s_2,r_2)=\delta_2\left\{\frac{\delta_2(s_2-r_2)}{4+\delta_2^2(s_2-r_2)^2}-\frac{12[\delta_2(s_2-r_2)-2f}{[4+\delta_2^2(s_2-r_2)^2]^2}+\frac{64[\delta_2(s_2-r_2)-2f]}{[4+\delta_2^2(s_2-r_2)^2]^3}\right\} \tag{28}$$

$$K_{12}(s_1,r_2)=a\delta_2\{-K_s(a(\delta_1s_1+\sigma_1),a(\delta_2r_2+\sigma_2))+fK_n(a(\delta_1s_1+\sigma_1),\ a(\delta_2r_2+\sigma_2))\} \tag{29}$$

$$K_{21}(s_2,r_1)=a\delta_1\{-K_s'(a(\delta_2s_2+\sigma_2),\ a(\delta_1r_1+\sigma_1))-fK_n(a(\delta_2s_2+\sigma_2),\ a(\delta_1r_1+\sigma_1))\}. \tag{30}$$

For the numerical integration of (25) and (26) we follow the method of numerical solution of Cauchy-type singular integral equations due to Erdogan and Gupta[6, 7].
Accordingly, we set

$$B_1(r_1)=\frac{(\kappa+1)P}{2\mu a}(1-r_1^2)^{1/2}\phi_1(r_1) \tag{31}$$

$$B_2(r_2)=\frac{(\kappa+1)P}{2\mu a}(1-r_2^2)^{1/2}\phi_2(r_2). \tag{32}$$

The discretized forms of (25) and (26) become

$$\sum_{i=1}^{n}\frac{(1-r_i^2)}{n+1}\left\{\left[\frac{1}{r_i-s_k}+K_{11}(s_k,r_i)\right]\phi_1(r_i)+K_{12}(s_k,r_i)\phi_2(r_i)\right\}$$
$$=\frac{f}{\lambda}+\frac{2}{\pi}\frac{\delta_1s_k+\sigma_1+f}{[(\delta_1s_k+\sigma_1)^2+1]^2},\quad k=1,2,\ldots n+1. \tag{33}$$

$$\sum_{i=1}^{n}\frac{(1-r_i^2)}{n+1}\left\{\left[\frac{1}{r_i-s_k}+K_{22}(s_k,r_i)\right]\phi_2(r_i)+K_{21}(s_k,r_i)\phi_1(r_i)\right\}$$
$$=-\frac{f}{\lambda}+\frac{2}{\pi}\frac{\delta_2s_k+\sigma_2-f}{[(\delta_2s_k+\sigma_2)^2+1]^2},\quad k=1,2,\ldots n+1 \tag{34}$$

where

$$r_i=\cos\left[\frac{i\pi}{n+1}\right],\quad i=1,\ldots n \tag{35}$$

$$s_k=\cos\left[\frac{\pi(2k-1)}{2(n+1)}\right],\quad k=1,\ldots n+1 \tag{36}$$

$$\lambda=P/p_0a. \tag{37}$$

Equations (33) and (34) incorporate the boundedness requirement for $B_1(r_1)$ and $B_2(r_2)$. The system of equations (33) and (34) is nonlinear in the parameters δ_1, σ_1, δ_2, σ_2. To simplify the iteration procedure, we first exchange the roles of δ_1 and λ, since λ appears linearly in the equations and can be eliminated from the system by using, for instance, the $(n/2)+1$ equation of (33) with n even. The $(n/2)+1$ equation of (34) is also isolated and used for the determination of δ_2 by iteration. Thus we have a system of $2n$ equations to be solved for the $2n$ unknowns $\phi_1(r_i)$ and $\phi_2(r_i)$, provided that σ_1 and σ_2 are given. The values of σ_1 and σ_2 must be chosen so that (12) and (13) are satisfied. Thus we must make initial guesses for the three parameters δ_2, σ_1, σ_2 and proceed by iteration. This is practically impossible unless there are some clues. The solutions assuming first a single slip zone to the left of P and then a single slip zone to the right of P are used to provide initial guesses. As long as the two slip zones are not very close together, this scheme works very well because there is little interaction between the zones. In addition, the equation used for δ_2 is insensitive to small variations of σ_1 and σ_2.

The computations were performed for $n=50$. Convergence was established for $n=30$. The quantities of particular interest D_1 and D_2 remained accurate to the sixth significant figure.

RESULTS AND DISCUSSION

The extent and location of the slip zones for various values of the coefficient of friction are shown in Fig. 2 as functions of the loading parameter λ. Notice that the zones start at symmetrical points, but as the force increases they grow mainly by extension to the right, i.e. by displacement of the leading edge of the zone in the direction of motion. The most striking curve is that for $f=0.125$ where the left zone extends under the point of application of the force and the right zone is correspondingly reduced at its trailing edge.

Figure 3 shows the shear extraction at the interface for $f=0.5$. Note the continuous transition of the trailing ends and the "hooks" at the leading ends. The corresponding normal tractions are shown in Fig. 4.

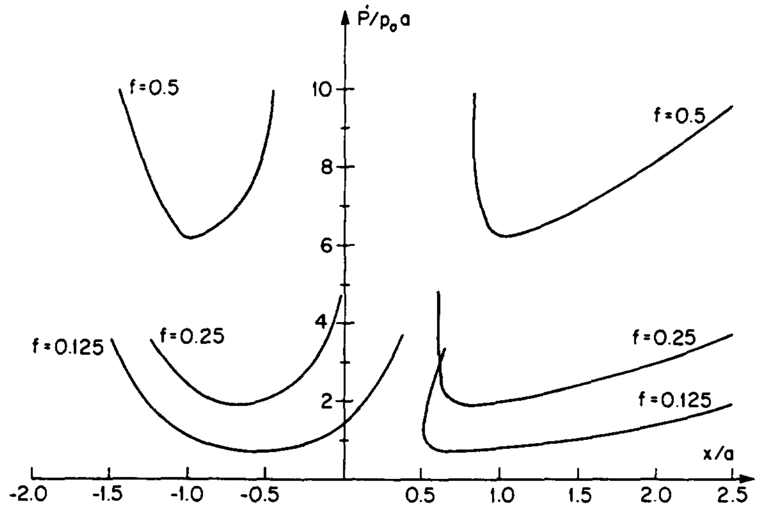

FIG. 2. Extent and location of slip zones vs load.

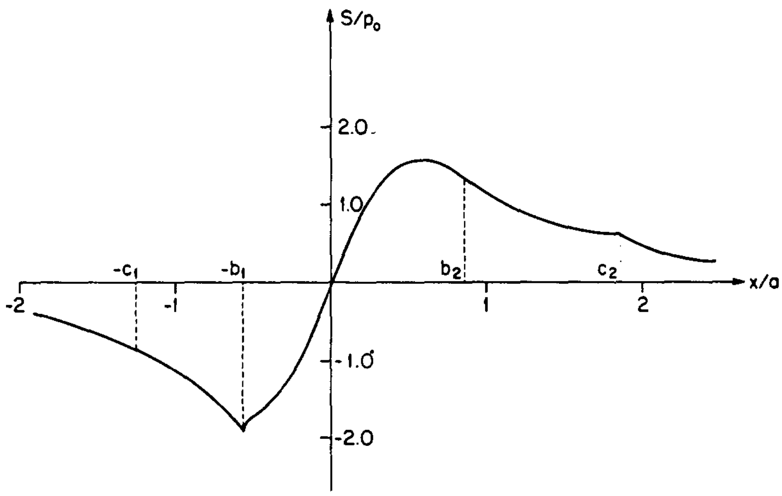

FIG. 3. Shear traction for $f = 0.5$.

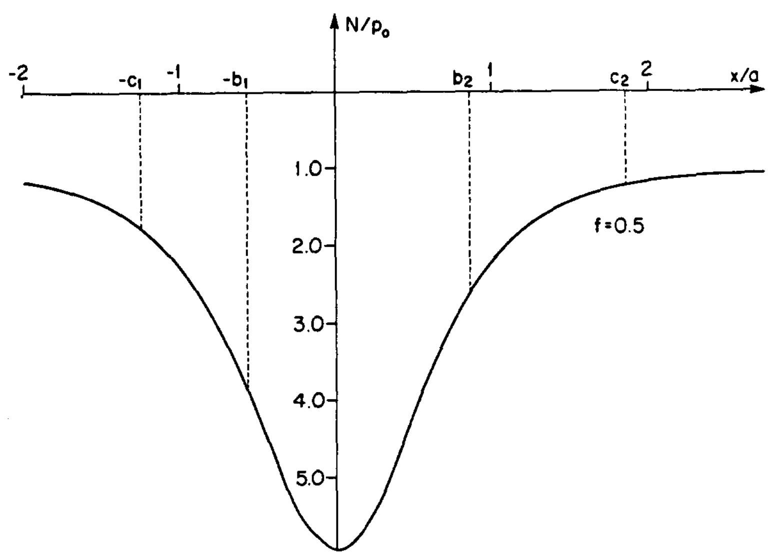

FIG. 4. Normal traction for $f = 0.5$.

Figure 5 shows the net tangential shifts D_1, D_2 for the two slip zones as functions of λ. We note that for $f = 0.5$, $|D_1| > |D_2|$ whereas for $f = 0.125$, $|D_2| > |D_1|$. In each case, the difference increases with increasing load and cannot be attributed to numerical error.

The slip in the two zones is opposite in sense, so that when we plot the total net shift $(D_1 + D_2)$ due to the passage of the load in Fig. 6, we find that it is positive for $f = 0.5$ and negative for $f = 0.125$. Thus, for high coefficients of friction, the layer creeps in the direction of motion of the load, whereas for low coefficients it creeps in the opposite direction. For an intermediate value, $f = 0.25$, we find that $(D_1 + D_2)$ is positive for loads just above the critical value for initiating slip, but negative for higher loads.

These results can be compared with a series of experiments by Anscombe and Johnson[5] on the rolling of two steel cylinders, one of which was fitted with a steel tire. The tire can be modelled as a layer supported by a substrate of similar material, and the interference fit between the tire and the core provides a normal pressure p_0 at the interface. The compressive force between the rollers during operation appears as a normal force moving over the surface of the tire.

Anscombe and Johnson observed that the tire creeps around the core in the opposite direction to the motion of the force and their results are compared with calculated values of $(D_1 + D_2)$ in Fig. 7. A direct comparison would require appropriate values of coefficient of friction and these are not available. Coefficients in the range 0.10–0.15 were estimated from the pressing force required during assembly, but Fig. 7 suggests that lower coefficients are appropriate for the interfacial slip due to the moving force. This is not unreasonable in view of the small amount of displacement which occurs at each passage of the load. Computationally, it is very difficult to obtain results with the present iteration scheme when the coefficient of friction is very low, because the two slip zones start to interact more strongly.

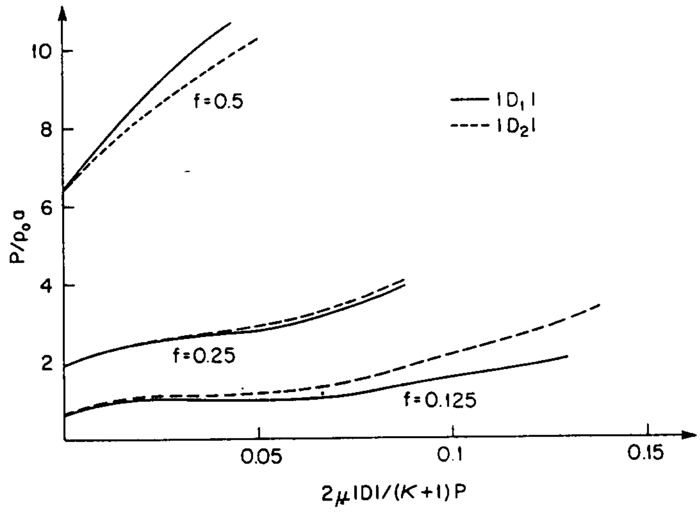

FIG. 5. Net tangential shifts for each zone vs load.

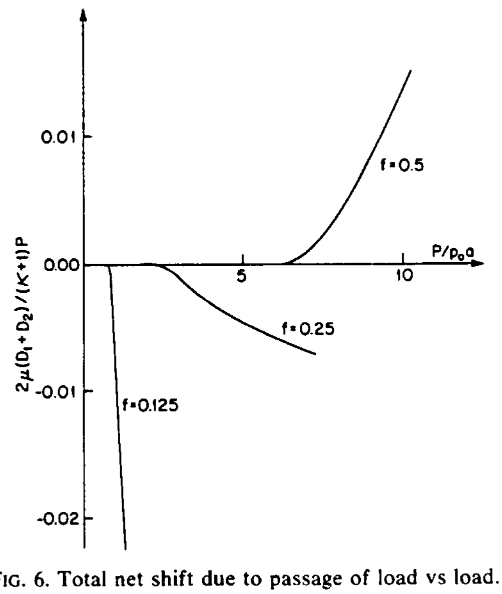

FIG. 6. Total net shift due to passage of load vs load.

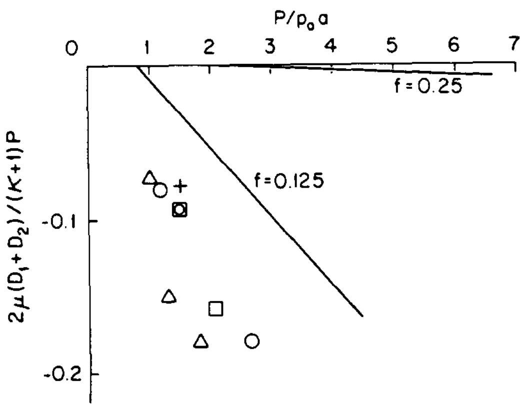

FIG. 7. Comparison with experimental results of [5].

Anscombe and Johnson also give a simple analytical treatment of the problem which does not model the physics of the process, but which gives good agreement if suitable coefficients of friction are chosen. The complex behavior uncovered by the present more rigorous analysis would seem to confirm their suspicion that this agreement is "partly fortuitous"!

Acknowledgement—Support by the National Science Foundation through the grant CME 8019281 is gratefully acknowledged.

REFERENCES

1. M. COMNINOU, D. SCHMUESER and J. DUNDURS, Fractional slip between a layer and a substrate caused by a normal load. *Int. J. Engng Sci.* **18**, 131–137 (1980).
2. D. SCHMUESER, M. COMNINOU and J. DUNDURS, Separation and slip between a layer and substrate caused by tensile load. *Int. J. Engng. Sci.* **18**, 1149–1155 (1980).
3. D. SCHMUESER, M. COMNINOU and J. DUNDURS, Frictional slip between a layer and a substrate. *J. Engng Mech. Div. ASCE* **109**, 1103–1118 (1981).
4. M. COMNINOU, J. R. BARBER and J. DUNDURS, Interface slip caused by a surface load moving at constant speed. *Int. J. Mech. Sci.* **24**.
5. H. ANSCOMBE and K. L. JOHNSON, Slip of a thin solid tyre press-fitted on a wheel. *Int. J. Mech. Sci.*, **16**, 329–334 (1974).
6. F. ERDOGAN and G. GUPTA, On the numerical solution of singular integral equations, *Quart. Appl. Math.* **30**, 525–534 (1972).
7. F. ERDOGAN, G. D. GUPTA and T. S. COOK, Numerical solutions of singular integral equations. In *Methods of Analysis and Solution of Crack Problems* (Edited by G. SIH). Noordhoff, Leyden (1973).